Solution of multi-channel problems using MCAS for spectra and scattering cross sections.

K. Amos [1], S. Karataglidis [1], P. Fraser [1], D. van der Knijff [2], J. P. Svenne [3], L. Canton [4], and G. Pisent [4]

February 9, 2008

Abstract

A multi-channel algebraic scattering theory, to find solutions of coupled-channel scattering problems with interactions determined by collective models, has been structured to ensure that the Pauli principle is not violated. Positive (scattering) and negative (sub-threshold) solutions can be found to predict both the compound nucleus sub-threshold spectrum and all resonances due to coupled-channel effects that occur on a smooth energy varying background. The role of the Pauli principle is crucial in defining what interaction potentials are required to fit data. The theory also gives an algebraic form for the dynamic polarization potential which adds to the ground state interaction to define the optical potential that gives the same elastic scattering cross sections.

1 Introduction

Low-energy cross sections from the collision of nucleons with light-mass nuclei show sharp as well as broad resonances upon a smooth, energy-dependent background. Those resonances may correlate to states in the discrete spectrum of the target. To interpret such scattering data requires use of a complex coupled-channel reaction theory . A theory with very important improvements over those used heretofore has been developed [1]. This theory, named a multi-channel algebraic scattering (MCAS) theory, finds solution of the coupled Lippmann-Schwinger equations for the quantum scattering of two fragments. Though the method can be applied to quite general scattering systems, to date studies have been limited to nucleon scattering from zero ground state spin targets.

The prime information sought are scattering (S-) matrices which are easily extracted from the T-matrices generated by MCAS. The approach involves using matrix algebra on matrices built using Sturmian-state expansions of the relevant nucleon-nucleus potential matrix. With this method, all resonances in any energy range can be identified, and their centroids, widths, and spin-parities determined as can the energies and spin-parities of sub-threshold states of the system.

It has long been known that collective-model prescriptions of nucleon-nucleus scattering violate the Pauli principle. However, the MCAS procedure enables use of an orthogonalizing pseudo-potential (OPP) approximation by which unphysical effects due to violation of the Pauli principle can be avoided. Doing so is crucial

[1]School of Physics, The University of Melbourne, Victoria 3010, Australia
[2]Advanced Research Computing, University of Melbourne, Victoria 3010, Australia
[3]Department of Physics and Astronomy, University of Manitoba, and Winnipeg Institute for Theoretical Physics, Winnipeg, Manitoba, Canada R3T 2N2
[4]Istituto Nazionale di Fisica Nucleare, Sezione di Padova, e Dipartimento di Fisica dell'Università di Padova, via Marzolo 8, Padova I-35131, Italia

to finding the parameter values of the interaction that simultaneously gives the sub-threshold spectrum and the low energy scattering cross sections [2].

The multichannel formalism and the process by which resonances can be identified and located are outlined next. Results of calculations made using a collective-model prescription for the potential matrix are then discussed. In that collective model, the interaction field is allowed to be deformed from sphericity and that deformation is taken to second order. In studies of nucleon scattering from ^{12}C, coupling is taken to the ground 0^+_1, 2^+_1 (4.4389 MeV), and 0^+_2 (7.6542 MeV) states and we consider nucleon energies to 6 MeV. With these three states defining the relevant target spectrum, only quadrupole deformation is involved. In a new development, we have applied the MCAS method to the p+^{6}He system and have compared results with the spectrum of ^{7}Li known from experiment.

The theory also allows the construction of the optical potential by appropriately subsuming the coupled-channel equations into effective elastic-channel scattering equations. The optical potentials thus constructed, as well as allowing for the Pauli principle, are very nonlocal and energy dependent. However, the potentials guarantee that their use lead to cross section details including resonance effects. We present typical results for the n+^{12}C case.

2 The MCAS theory (in brief)

The integral equation approach to scattering in momentum space for potential matrices $V^{J^\pi}_{cc'}(p,q)$ where $c = [(\ell s)j, IJ^\pi]$ where J^π are conserved quantum numbers which will often be omitted for convenience, requires solution of coupled Lippmann-Schwinger (LS) equations giving a (partial wave) multichannel T-matrix of the form

$$T_{cc'}(p,q;E) \;=\; V_{cc'}(p,q) + \frac{2\mu}{\hbar^2}\left[\sum_{c''=1}^{\rm open}\int_0^\infty V_{cc''}(p,x)\frac{x^2}{k^2_{c''}-x^2+i\epsilon}T_{c''c'}(x,q;E)\;dx \right. \\ \left. - \sum_{c''=1}^{\rm closed}\int_0^\infty V_{cc''}(p,x)\frac{x^2}{h^2_{c''}+x^2}T_{c''c'}(x,q;E)\;dx\right] \;. \quad (1)$$

The open and closed channels contributions have channel wave numbers $k_c = \sqrt{\frac{2\mu}{\hbar^2}(E-\epsilon_c)}$ and $h_c = \sqrt{\frac{2\mu}{\hbar^2}(\epsilon_c - E)}$, for $E > \epsilon_c$ and $E < \epsilon_c$ respectively. ϵ_c is the threshold energy of the target state inherent in channel c and μ is the reduced mass. Solutions of Eq. (1) are sought using expansions of chosen model potential matrix elements in (finite) sums of energy-independent separable terms,

$$V_{cc'}(p,q) \sim \sum_{n=1}^{N} \chi_{cn}(p)\;\eta_n^{-1}\;\chi_{c'n}(q)\;. \quad (2)$$

In the MCAS method [1], the form factors are specified in terms of a set (n) of Sturmians $\Phi_{c,n}(p)$ via

$$|\chi_{c,n}\rangle = \sum_{c'} V_{cc'}\,|\Phi_{c,n}\rangle\;, \quad (3)$$

and the Sturmians themselves are solutions of coupled-channel (Schrödinger) equations for the chosen matrix of potentials $V_{cc'}(p,q)$ with eigenvalues η_n.

In coordinate space those potentials are defined using a collective model prescription for the nucleon-target system, with local forms $V_{cc'}(r)$. The Pauli principle can be satisfied by using an OPP method in the determination of the Sturmians. Those Sturmians then are solutions of coupled-channel equations for the matrix of nonlocal potentials

$$\mathcal{V}_{cc'}(r,r') = V_{cc'}(r)\delta(r-r') \;+\; \lambda A_c(r)A_c(r')\,\delta_{cc'}\;, \quad (4)$$

where $A(r)$ is the radial part of the single particle (bound) state wave function in channel c spanning the phase space excluded by the Pauli principle. The OPP method holds in the limit $\lambda \to \infty$, but use of $\lambda = 1000$ MeV suffices.

The link between the multichannel T- and S-matrices is $S_{cc'} = \delta_{cc'} - i\pi \frac{2\mu}{\hbar^2} \sqrt{k_c k_{c'}}\, T_{cc'}$ which expands in matrix form with the Sturmians as the basis set to

$$S_{cc'} = \delta_{cc'} - i^{l_{c'}-l_c+1} \frac{2\mu\pi}{\hbar^2} \sum_{n,n'=1}^{N} \sqrt{k_c}\chi_{cn}(k_c) \left([\boldsymbol{\eta} - \mathbf{G}_0]^{-1} \right)_{nn'} \chi_{c'n'}(k_{c'}) \sqrt{k_{c'}} \ , \quad (5)$$

where now c, c' refer to open channels only. In this representation, $\boldsymbol{\eta}$ has matrix elements $(\eta)_{nn'} = \eta_n \ \delta_{nn'}$ while $\mathbf{G}_0$ has elements

$$\begin{aligned} (G_0)_{nn'} \quad = \quad & \frac{2\mu}{\hbar^2} \left[\sum_{c=1}^{\text{open}} \int_0^\infty \chi_{cn}(x) \frac{x^2}{k_c^2 - x^2 + i\epsilon} \chi_{cn'}(x) \ dx \right. \\ & \left. - \sum_{c=1}^{\text{closed}} \int_0^\infty \chi_{cn}(x) \frac{x^2}{h_c^2 + x^2} \chi_{cn'}(x) \ dx \right] \ . \end{aligned} \quad (6)$$

The bound states of the compound system are defined by the zeros of the matrix determinant when the energy is $E < 0$ and so link to the zeros of $\{|\boldsymbol{\eta} - \mathbf{G}_0|\}$ when all channels in Eq. (6) are closed.

The Sturmian expansions and their use have been detailed recently [1] and are not repeated herein. Suffice it to note that a finite set can be used to make the expansion of finite rank. An essential feature in such studies, if very narrow resonances are to be observed, is a resonance finding scheme. Such is also given in detail in Ref. [1]. Essentially that requires recasting the elastic scattering S-matrix (for each J^π and with the elastic channel taken as $c = 1$) as

$$S_{11} = 1 - i\pi \frac{2\mu}{\hbar^2} \sum_{nn'=1}^{M} k \ \chi_{1n}(k) \frac{1}{\sqrt{\eta_n}} \left[\left(\mathbf{1} - \boldsymbol{\eta}^{-\frac{1}{2}} \mathbf{G}_0 \boldsymbol{\eta}^{-\frac{1}{2}} \right)^{-1} \right]_{nn'} \frac{1}{\sqrt{\eta_{n'}}} \chi_{1n'}(k) \, . \quad (7)$$

Here, the elements of the diagonal (complex) matrix $\boldsymbol{\eta}^{-\frac{1}{2}}$ are $\frac{1}{\sqrt{\eta_n}} \delta_{nn'}$. Then the complex-symmetric matrix, $\boldsymbol{\eta}^{-\frac{1}{2}} \mathbf{G}_0 \ \boldsymbol{\eta}^{\ -\frac{1}{2}}$ can be diagonalized and the evolution of its complex eigenvalues ζ_r with respect to energy, define resonance attributes. Resonant behavior occurs when one of the complex ζ_r eigenvalues passes close to the point $(1, 0)$ in the Gauss plane. At the energy corresponding to that point, the elastic channel S-matrix has a pole.

3 Results using MCAS for n and $p + {}^{12}\mathbf{C}$

The MCAS approach has many advantages over the more usual coordinate space solution methods. Notably with it one can 1) account for the effects of the Pauli principle, even for collective model descriptions of the coupling potentials, 2) specify sub-threshold states in the compound nucleus, 3) locate all resonances caused by $V_{cc'}(r)$ and find their centroid energies and widths in the energy range chosen, no matter how small their widths, and 4) specify the complete T- and S-matrices off-shell enabling prediction of all low energy elastic and inelastic cross sections and spin observables.

3.1 A comparative study

In this first subsection, we present the results from a comparative study of a coordinate space program with MCAS (with and without taking into account the Pauli

principle). We seek to see if, when one performs as exactly the same evaluation as possible, the calculations are equivalent. Also, for a typical low energy problem, we ask how the Pauli principle influences the results.

To make a "fair" comparison, we have used a simplified model for the n+^{12}C system. We chose the same three target states to define the coupled channels in both the coordinate-space (ECIS97 [3]) and momentum-space (MCAS) evaluations. For this we take coupling to be effected by a simple rotational model scheme having only a quadrupole deformation, $\beta_2 = -0.52$, on the real potential [3],

$$V(r) = -49.92\, f(r) \,+\, \left(\frac{\hbar}{m_\pi c}\right)^2 6\,\sigma\cdot\nabla f(r) \times \frac{1}{i}\nabla; \quad f(r) = \left[1 + e^{\left(\frac{r-2.885}{0.63}\right)}\right]^{-1}. \tag{8}$$

The potential units are MeV and all lengths are in fm. In the MCAS evaluation, however, the spin-orbit term is reduced to the $\mathbf{l}\cdot\mathbf{s}$ form. Doing so has little effect on elastic scattering [5]. Initial runs of ECIS97 for the simplified model were for (lab.) energies from 0.1 MeV to 4.0 MeV in steps of 0.1 MeV. Those results indicated that there were three resonances near 0.7, 2.1, and 3.3 MeV. Thus additional calculations were made for more closely spaced energies spanning those three values and the results are displayed by the filled circles in Fig. 1.

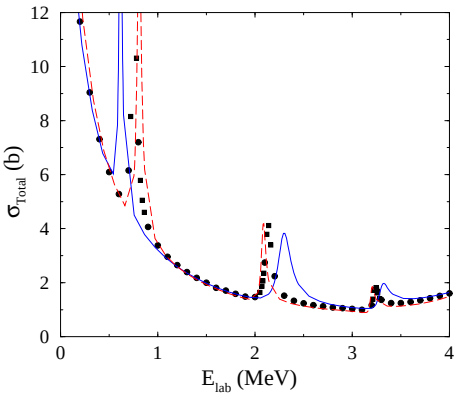

Figure 1: The n+^{12}C cross section results from using MCAS theory with those found using the ECIS approach. Details are given in the text.

Therein they are compared with the results of MCAS calculations, using the same simplified model and, essentially, the fixed interaction given in Eq. (8), but without accounting for the Pauli principle. The solid curve is the MCAS result when the deformation (of $V_{cc'}$) was taken through second order [1, 4]. The three resonances seen in the ECIS results are present though their energy centroids are slightly shifted. But the background on which those resonances lie agrees very well with the ECIS result. The second MCAS result (dashed curve) was obtained by limiting deformation to first order and now the agreement with the ECIS result is much better for both background and the resonances; centroids and widths.

We draw two conclusions. First when the simplified model is used in exactly the same way in finding solutions of the coupled-channel problem using the coordinate-space approach [3] and the momentum-space approach with MCAS [1], the scattering cross sections agree very well. The smooth background as well as the specific resonances that can be generated with ECIS are found with the MCAS run. Those were calculations with deformation taken to first order. The second conclusion from comparison of the two MCAS results is that, with deformation of -0.52 in the n+^{12}C system, expansion of $V_{cc'}$ need be taken to second order.

However, all of the calculations ignored the effects of the Pauli principle [2]. But in the MCAS approach, the OPP method can be used to ensure that there is no violation of the Pauli principle even when a collective model is used to specify the interaction potentials. The OPP method constrains the Sturmians used as an expansion set are orthogonal to all states in which the incoming nucleon would be trapped into an orbit fully occupied by nucleons in the target. Using such a conditioned Sturmian function set to solve the MCAS theory of coupled equations

gave the cross section displayed by the solid curve in Fig. 2. There is a considerable change in the resonances observed though the background cross section, being dominated by s-wave scattering, is little varied.

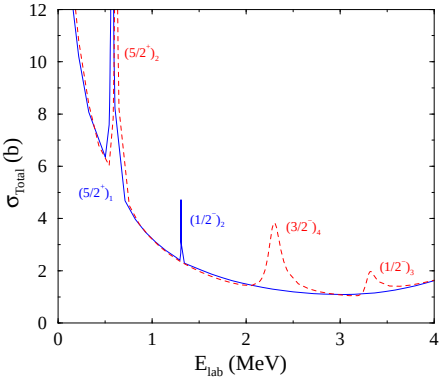

Figure 2: The n+^{12}C cross section results from using MCAS theory with (solid curve) and without (dashed curve) using the OPP method.

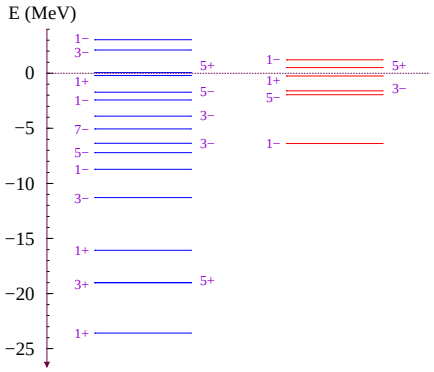

Figure 3: The n+^{12}C sub-threshold (and resonance) spectra found using MCAS with (right) and without (left) accounting for the Pauli principle.

The number of resonances drops from three to two in this energy range when the Pauli principle is considered. Further, those resonances inherently have different underlying structures, as the $\frac{5}{2}^+$ resonance with centroid near 0.6 MeV is of rank 1 and not 2 when the Pauli principle is considered. (Here by rank we mean the number of the state of given J^π in ^{13}C.) Likewise the $\frac{1}{2}^-$ resonance, in addition to being shifted in position by some 2 MeV, has a smaller width and is of rank 2.

The MCAS method can be used with negative energies and so produce the sub-threshold compound nucleus bound state spectrum. With the fixed interaction of Eq. (8), the spectra (including the resonance states) found with and without using the OPP are shown on the right and left of Fig. 3 respectively. If the Pauli principle is violated, a large number of spurious states result.

3.2 Resonance finding

With MCAS, all resonances (spin-parity, centroid, width) can be found without requiring use of an inordinately large number of energy values. The procedure is to solve the matrix equations for the eigenvalues $\zeta_r(E_i)$ for a (finite) set of energies. The energy centroid of a resonance is that value at which the eigenvalue track passes close to the point (1,0). Those eigenvalues are complex and their imaginary part relates to the resonance width [1]. A sample set of the eigenvalues for $\frac{3}{2}^+$ resonances in the n+^{12}C system generated using this method are shown in Fig. 4. The point values of the largest eigenvalue (labeled (1)) has been connected by a long-dashed line to guide the eye to link the energy sequence of the results. The actual trajectory has a cusp. That is very evident with curve (1), but similar though more slight features are evident in the trajectories (2) and (3). That cusp feature of the eigenvalue trajectories links to the opening of the 2^+_1 state at 4.4389 MeV in the coupled-channel algebra. Note that these eigenvalues have small imaginary parts and so the plot is semi-logarithmic. Thus some details of the trajectories lie below the graphed range. The largest eigenvalue clearly evolves well beyond the unit circle after crossing at the energy of the lowest $\frac{3}{2}^+$ compound resonance in this cross section. That centroid is located at 3.0 MeV. The imaginary part is consistent with the width. Next note

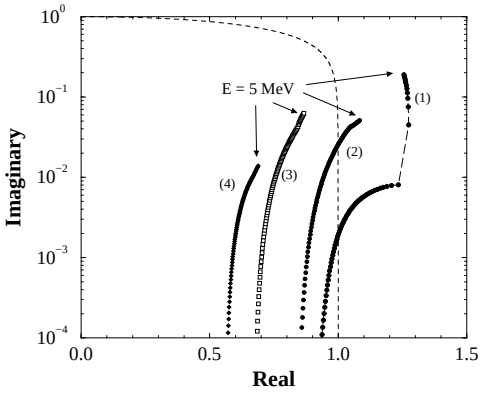

that the 2nd trajectory crosses the unit circle at higher energy and with a larger imaginary part. This coincides with a second, broader, $\frac{3}{2}^+$ resonance at 3.4 MeV. The 3rd and 4th Sturmian trajectories shown track toward the unit circle but have not crossed before 5 MeV. In this way all resonances of all the spin-parities considered are always found, no matter how narrow they are.

Figure 4: Argand plots of $\frac{3}{2}^+$ resonance finding eigenvalues for the n+^{12}C system. The dashed line is the unit circle.

3.3 Cross sections and sub-threshold states

Results of our MCAS study of the neutron plus ^{12}C system for excitation in ^{13}C to $\sim$ 10 MeV, are displayed in Fig. 5. The interaction potential parameters used were those tabulated in Ref. [2]. In this figure, the elastic scattering cross section is compared with data with respect to the ground state of ^{12}C as zero energy. On the same scale, in the right hand parts of the figure, we compare the experimental with theoretical sub-threshold and

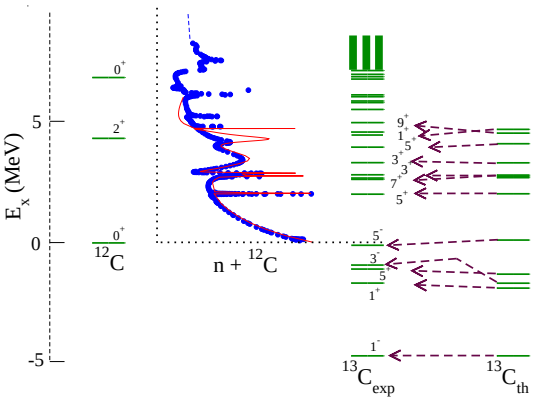

Figure 5: Spectra of ^{12,13}C and the elastic cross section for the n+^{12}C system.

resonance states in ^{13}C. The labels denote values of $2J$ and parity.

That same elastic cross section and MCAS result are shown in the top panel of Fig. 6 with the bottom two panels showing what using the S-matrices give as predictions of polarizations at two scattering angles. The resonance structures most evident in the cross section are well reproduced by MCAS and those details are confirmed in the polarizations. The spin-parities of the resonances also coincide with those of known states in the spectrum of ^{13}N. Notably the prominent $\frac{5}{2}^+$ resonance at 2 MeV, and the two $\frac{3}{2}^+$ resonances spanning 2.8 - 4.0 MeV, are found with very good widths, narrow and broad respectively. In Fig. 7, proton scattering cross sections (from ^{12}C) is shown at two scattering angles. Found simply by adding a Coulomb potential to the n+^{12}C system interactions, the results from MCAS calculations (of p-^{12}C scattering) compare well with the data.

3.4 The spectra of ^{7}Li from the p+^{6}He system

MCAS results for the p+^{6}He system have been found when the target (^{6}He) structure is taken as three states; the 0^+ (ground), and two 2^+ states at 1.78 and 5.68

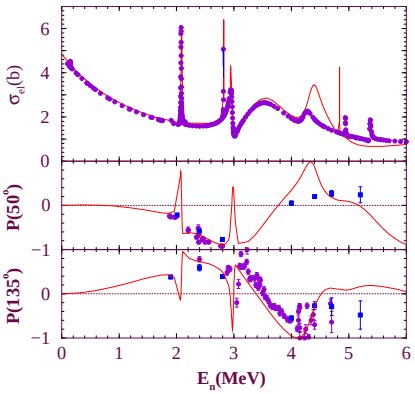

Figure 6: The elastic cross section for n-^{12}C scattering (top) and polarizations at 50° (middle) and at 135° (bottom).

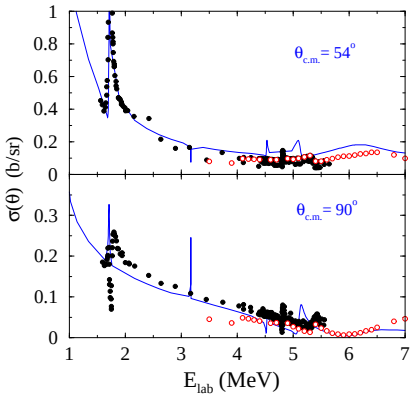

Figure 7: MCAS predictions and proton scattering cross-section data at two fixed scattering angles.

MeV respectively. A quadrupole deformation was considered and both 2^+ states were allowed to couple to the ground with the same deformation and between each other through second order. To get the results displayed in Fig. 8, the input interaction potential required a large diffuseness consistent with the target having an extended neutron matter distribution. The results on the far left in Fig. 8, were found with the deformation set to zero. They show the sub-structural origins of each state in the actual spectrum [4]. Again use of the OPP to account for Pauli blocking of occupied states was crucial in finding these results. With zero deformation then states reduce to those of a bound proton to one of the three states of ^{6}He. The ground state is a $0p_{3/2}$ proton bound to the ^{6}He ground and 1.8 MeV above that there is the quadruplet of states formed by such a proton bound to the first excited (2^+) state. That is also the case for the quadruplet 5.6 MeV above the ground and due to coupling to the second excited (2^+) state. The single state remaining is that of a $0p_{1/2}$ proton bound to the ground. With non-zero deformation, these states mix and spread to give the theoretical set that compare quite favorably with those known from experiment for ^{7}Li. Evaluating the n+^{6}He system, one would expect more sub-threshold states, as is the case with the mass 13 systems.

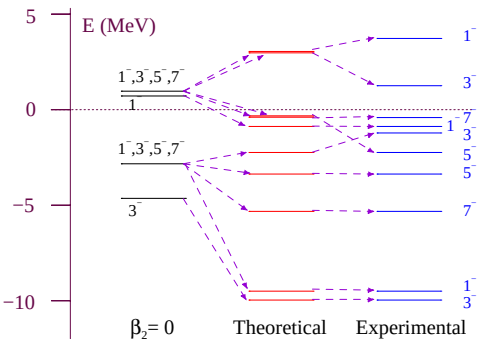

However, one also has to alter the OPP since there is a (partial at least) new blocking of the $0p$-shell. The MCAS result for the particle-unstable nucleus ^{7}He gives one weakly-bound state. A slight adjustment of the interaction chosen would move that state into the continuum without seriously changing the ^{7}Li results.

Figure 8: The spectra of ^{7}Li as determined using MCAS for the p+^{6}He system.

4 MCAS and the optical potential

Assuming a local form for the elastic channel element of the potential matrix in the MCAS approach, and with the operator

$$\mathbf{\Lambda}(E) = \left[\eta - \mathbf{G}_0^{(Q)}(E)\right]^{-1} - \eta^{-1} \ , \qquad (9)$$

involving the free Green function excluding the elastic channel, the optical potential for elastic scattering takes the nonlocal form [1] with the addition of

$$\Delta U(r,r';E) = \sum_{n,n'=1}^{N} \chi_{1n}(r)\,[\mathbf{\Lambda}(E)]_{nn'}\,(E)\chi_{1n'}(r')\ , \tag{10}$$

to $V_{11}(r)$. Here $\chi_{1n}(r)$ are Bessel transforms of the form factors $\chi_{1n}(k)$ and ΔU is known as the dynamic polarization potential (DPP). At low energies it is this makes the formulated optical potential complex (if the energy allows more than one open channel), nonlocal, and energy dependent. The DPP has been calculated using the MCAS approach and values of them found for 2.73 MeV neutrons on ^{12}C are plotted in Fig. 9 for three partial waves, $\ell = 0, 1, 2$. The central depths of each are indicated on the right as are the energy steps of the contour lines. As the energy is below the first inelastic threshold, the DPP is purely real. But the coupled-channel effects make that aspect of the optical potential extremely nonlocal. The DPP is also very angular momentum dependent. Of course for energies above 4.4389 MeV, the DPP becomes complex since the threshold for the first inelastic scattering has been exceeded.

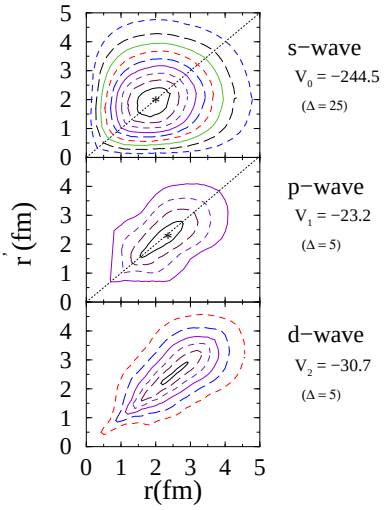

Figure 9: The DPP (MeV-fm^{-1}) for three partial waves for 2.73 MeV neutrons from ^{12}C

5 Conclusions

The MCAS approach to analyze (low-energy) nucleon-nucleus scattering is built from a model structure of the interaction potentials between a nucleon and each of the target states taken into consideration. All resonances (narrow and broad) in the cross section within the selected (positive) energy range can be found on a background. With negative energies, the MCAS method specifies the sub-threshold bound states of the compound nucleus. The scheme allows for a resonance finding procedure by which all resonances (and sub-threshold bound) states will be found within a chosen energy range. Further via use of the OPP in definition of the Sturmians to be used, those functions are assured to be orthogonal to any single nucleon bound state that is Pauli blocked. That allowance for the influence of the Pauli principle is crucial in finding results that concur well with observation.

References

[1] K. Amos *et al.*, Nucl. Phys.**A728**, 65 (2003).

[2] L. Canton *et al.*, Phys. Rev. Lett. **94**, 122503 (2005).

[3] J. Raynal, *Notes on ECIS94*, CEA Saclay report No. CEA-N-2772, (1994).

[4] G. Pisent, *et al.*, Phys. Rev. C **72**, 014601 (2005).

[5] K. Amos *et al.*, submitted for publication in Phys. Rev. C. (2005).